Rheology of PA-6/EPM/EPM-gMA Blends Along a Twin-Screw Extruder

J. A. COVAS and A. V. MACHADO

Department of Polymer Engineering, University of Minho, 4800 Guimarães, Portugal

M. VAN DUIN

DSM Research, P.O. Box 18, 6160 MD Geleen, The Netherlands

Abstract

The changes in the rheological behavior, morphology, and chemical conversion of PA-6/EPM/EPM-g-MA blends (80/20/0 to 80/0/20; w/w/w) along a compounding co-rotating twin-screw extruder were monitored. The linear viscoelastic behavior of nonreactive and reactive blends could be interpreted in terms of morphology and/or chemical conversion. However, a quantitative prediction of the rheological response using Lee and Park's theory, which relates the rheological behavior with morphological changes of polymer blends, taking into account coalescence and breakup phenomena, was not possible because of the observed degradation of PA-6 along the screw. Matrix degradation also explains the low viscosity levels of the blends when compared with those of the original materials.

Introduction

Blending (immiscible) polymers has successfully been used as an alternative route for synthetic approaches to develop materials with an improved performance for specific applications. [1−5] In

these type of blends, a two-phase material is typically obtained, where droplets of one polymer (dispersed phase) are embedded in a matrix of another polymer (continuous phase). Interfacial tension induces a spherical drop shape under static conditions, although other parameters, such as the rheological properties of each component, are also relevant. The characteristics of immiscible polymer blends are determined by the blend composition, the properties of the individual components, and the morphology generated (i.e., which polymer is the matrix/dispersed phase and what is the size of the dispersed domains). The blend morphology is dictated by the interfacial interactions, the rheological properties of the components, and the kinetics of the relevant chemical and physical processes. Compatibilization of heterogeneous blends is generally used to control the interfacial properties and to stabilize the morphology against

coalescence and, thus, affects the equilibrium degree of dispersion. Compatibilization is generally accomplished by either adding a pre-synthesized block copolymer or via reactive processing. [2–5] In the latter case, the compatibilizer is generated in-situ, during blending, via grafting or exchange reactions. These reactions must generate sufficient copolymer in order to optimize the morphology and, thus, the blend performance. Since the reactions occur across phase boundaries, high stresses must be applied to enlarge the interfacial area and ensure high reaction rates.

Considerable effort has been devoted to identify and understand the mechanisms that govern chemical conversion and/or morphology development during blending. Emulsions of low viscous liquids were initially studied both experimentally and theoretically to simulate the two-phase morphology of blends. Several on- and off-line techniques, such as microscopy, spectroscopy, molecular weight, and rheology measurements, have been used successfully for blend characterization. [5] If correlations between rheological behavior and blend morphology could be established, rheology could be used as a sensitive tool to monitor and control morphological changes.

The linear viscoelastic response of nonreactive blends under small amplitude oscillations has been used extensively to characterize the microscopic structure of the material, provided the morphology is stable and no degradation occurs. [6–14] An increase in elasticity at low frequencies has been consistently reported and is usually attributed to the deformation of the dispersed particles and the recovery to their equilibrium shape due to interfacial tension. [6–9] This type of measurement is also very sensitive to the volume fraction and the copolymer nature. Palierne [15] developed a model accounting for this type of dynamic mechanical response of concentrated emulsions, where the deformation of the droplets and interfacial tension was considered. Large deformation flows can affect the blend morphology by deforming the dispersed phase. Also, during blending, coalescence and breakup take place, depending on the composition and strain.

Thus, the applied flow history will change the blend morphology (and consequently the rheological behavior); that is, the rheological properties measured are no longer characteristic of a specific morphology, but they reflect changes in morphology caused by flow. [10] Doi and Ohta [16] derived a constitutive equation for a blend of two immiscible Newtonian fluids with equal viscosity considering the latter phenomena. Later, Lee and Park [17] accounted for the effect of the viscosity ratio of the blend components.

Since the Palierne and the Doi-Ohta models predict quite different rheological characteristics, each has been used with relative success to describe the behavior of, for example, immiscible blends of polyisoprene with polydimethylsiloxane with different viscosity ratios, [7,11] polyethene with polystyrene, polyethyleneterephthalate with poly(ethene-covinylacetate), polypropylene with poly(ethene-covinylacetate) [12] and poly(methyl metacrylate) with acrylic impact modifiers. [13] Transient flow experiments involving, for example, a step-up in the initial low shear rate followed by flow reversal, seem to be particularly suited to evaluate the potential of the models mentioned and of their extensions to predict flow-induced changes in morphology. [10,11]

Only a very small number of authors have used rheological measurements as a tool to monitor the chemical conversion in reactive blends (see, e.g., references 19-21). Generally, capillary pressure drop and oscillatory measurements have shown that interfacial adhesion-thus, blend viscosity-increases with increasing amounts of copolymer formed at the interface. [19–21]

Most of the above studies examined the blend morphology and the rheological behavior of samples previously prepared in extruders or batch mixers. Another approach has consisted of monitoring on-line the development of morphology (and corresponding rheology changes) of simple model blends under controlled flow conditions (see, e.g., references 13 and 23). Specific on-line techniques for monitoring the microstructure of polymer blends were developed by Sakai [24] and Esseghir et al. [25] However, the specific problem of the evolution of the characteristics of immiscible blends during their preparation under conditions relevant to the industrial practice has seldom been addressed. [19] This is associated with the practical difficulty in carrying out in-line measurements or in collecting representative samples for subsequent testing.

The objective of this work is to monitor the evolution of the rheological parameters of immiscible, reactive polymer blends during extrusion, and to

RHEOLOGY OF PA-6/EPM/EPM-g-MA BLENDS ALONG A TWIN-SCREW EXTRUDER

correlate the rheological behavior with the morphology evolution and chemical conversion along the extruder. Blends with varying compositions were prepared in a laboratorial intermeshing co-rotating twin-screw extruder, and representative samples were collected along the screw axis for subsequent characterization using a recently developed sampling device. [26] Measurements under small amplitude oscillatory flow were carried out in order to avoid unwanted morphology changes and/or material degradation (as checked by Scholz et al. [23]). Blends of polyamide-6 (PA-6), ethene-propene rubber (EPM), and EPM modified with maleic anhydride (MA) (EPM-g-MA) were selected for this purpose, given their industrial relevance. [1–5]

Experimental

MATERIALS

Commercial polyamide-6 (PA-6 Akulon® K123); ethene-propene rubber (EPM Keltan® 740) produced by DSM, the Netherlands; and ethene-propene rubber modified with maleic anhydride (EPM-g-MA Exxelor VA 1801, containing 0.49wt% of MA, as determined by FT-IR) provided by Exxon, Spain, were selected for this work. Table I defines the composition of the various blends. The PA-6 content was kept constant in all blends, but the amount of modified rubber was varied in order to start with

TABLE I
Composition of the PA-6/EPM/EPM-g-MA Blends

Blend (w/w/w)	EPM-g-MA (wt%)[a]	MA content of rubber phase (wt%)[a]

80/20/0	0	0
80/15/5	5	0.13
80/10/10	10	0.25
80/5/15	15	0.37
80/0/20	20	0.49

[aMA] content of EPM-g-MA is 0.49wt%; MA content of the rubber phase is the weight average of the combined EPM and EPM-g-MA rubber phase.

different amounts of maleic anhydride in each blend. PA-6 was dried for 16 h at 110°C before extrusion.

TWIN-SCREW EXTRUSION

The various blends of Table I were processed in a laboratory modular Leistritz LSM 30.34 intermeshing co-rotating twin-screw extruder under identical processing conditions. Figure 1 shows the extruder layout and the operating conditions selected. The screws have three mixing zones. The first comprises staggering kneading blocks offset 90° and a left element downstream. The second contains staggering blocks at 90° and −30°. Finally, the third mixing zone uses staggering blocks at −60° and 90°. The intensive mixing and heat transfer generated in

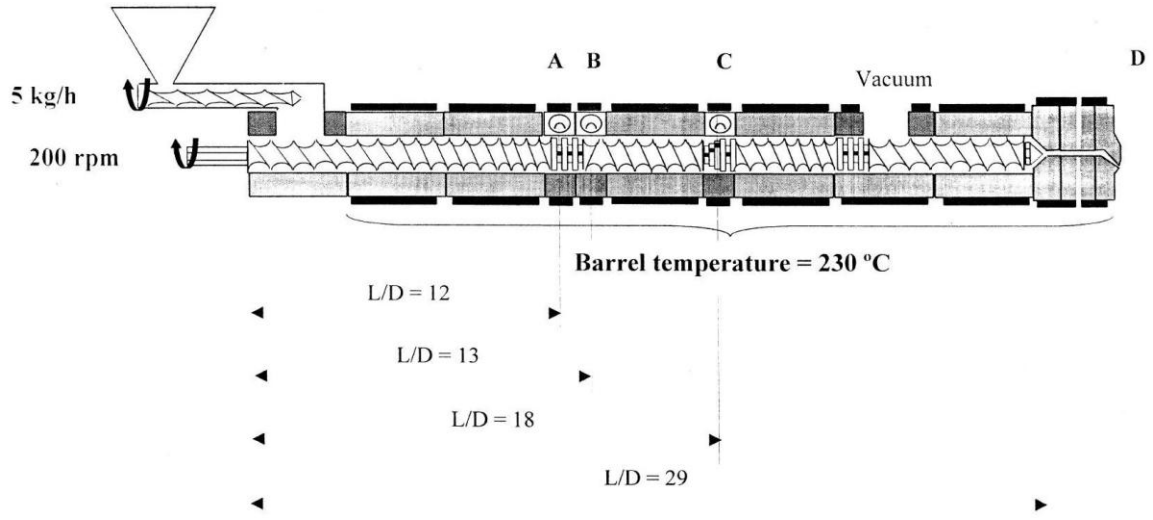

FIGURE 1. Extruder layout and sampling locations.

the first section will ensure complete material melting. Further mixing is induced upon flow through the subsequent mixing sections. Material samples were collected at the locations also indicated in Figure 1, through the use of sampling devices that were able to remove within 2 – 3 s circa 1 g of material from the extruder. [26] The samples were immediately quenched in liquid nitrogen, in order to avoid further reaction or morphological changes. The devices use the melt detour concept and can be inserted

between the barrel segments or, alternatively, barrel segments can be replaced by several adjacent collecting units. This provides the possibility of obtaining polymer samples at relatively small increments along the length of the screw.

MATERIALS CHARACTERIZATION

The details of the chemical and morphological characterization of the blends are given elsewhere. [27] Generally, after extracting all free PA6, the nitrogen content of the residues was determined. Blends were also hydrolyzed with hydrochloric acid in order to degrade the PA chains (amide functions) of the copolymer. The infrared spectra of the residue allowed the quantitative determination of the MA content of the samples using the anhydride carbonyl peak at $1785\ cm^{-1}$. The samples were either fractured in liquid nitrogen, etched with xylene to remove the rubber from the surface and observed with a Jeol JSM 6310F scanning electron microscope, or cryo-cut and analyzed with a Philips EM420 transmission electron microscope. The average size and the particle size distribution of the dispersed phase were estimated from the equivalent particle area of individual particles, which was measured with a Leica Quantimet 550 Image Analysis System.

The average molecular weight and the molecular weight distribution of PA-6 were determined using gel permeation chromatography. Samples were dissolved in 1,1,1,3,3,3-hexafluoro-i-propanol and then the solutions were analyzed in a Hewlett Packard 1090 M chromatograph with differential viscosimeter detector, at room temperature.

A few rheology experiments at high shear rates ($50 - 30{,}000\ s^{-1}$) were carried out using a Rosand RH7-2 twin-bore capillary rheometer. Viscosity measurements were performed at $230°C$, using two $1 - mm$ diameter dies (with L/D equal to 0.25 and 16) in order to carry out the Bagley correction for the end effects. The Rabinowitsch correction was performed to obtain the true shear rate. The material was preheated in the rheometer for 10 min , prior to each experiment.

Frequency sweeps (from 4×10^{-3} to 40 Hz) at $230°C$ were performed on a TA Instruments Weissenberg rheometer, using parallel-plate geometry (diameter = 40 mm) with a $2.00 - mm$ gap. A linearity check confirmed that strains up to 0.01 would keep the material's response in the linear viscoelastic domain. Before any experiment, samples were vacuum dried at $80°C$ during 12 h . The $1 - 2 - g$ nut-shaped samples collected from the extruder were compression molded for 10 min at $230°C$ under a pressure of 30 ton into discs $4 - cm$ wide and $2 - mm$ thick.

The possibility of three sources of error affecting the rheological data due to unwanted changes in morphology/chemistry during sample preparation or testing was initially considered. First, removing material from the extruder could affect the morphology due to flow through the sampling device and subsequent coalescence before cooling. In a separate study, [26] we confronted this new technique with conventional screw-pulling experiments. The experiments showed that in the case of PA-6/EPM blending, the samples collected with the devices exhibited smaller particles and narrower particle distributions; that is, coalescence was avoided. Also, shear rates in the sampling device were negligible.

The limited melt flow during compression molding increases the interfacial area and could therefore induce morphological and/or chemical conversion changes. However, as shown

in Table II, the morphology of nonreactive blend samples removed from the extruder remained unaffected regardless of the subsequent compression time.

Finally, although oscillatory measurements are commonly considered as a nondestructive technique for studying morphology/rheology correlations, the validity of this assumption was checked. Figure 2 (top) shows that no significant degradation

TABLE II
Dispersed Rubber Particle Size (Distribution) of PA-6/EPM (80/20; w/w) Blend for Different Compression Times

Compression time (min)	Particle size	
	Average (μm)	Variance (μm^2)
0	9.2	94
5	9.6	102
10	9.9	94
15	9.3	98

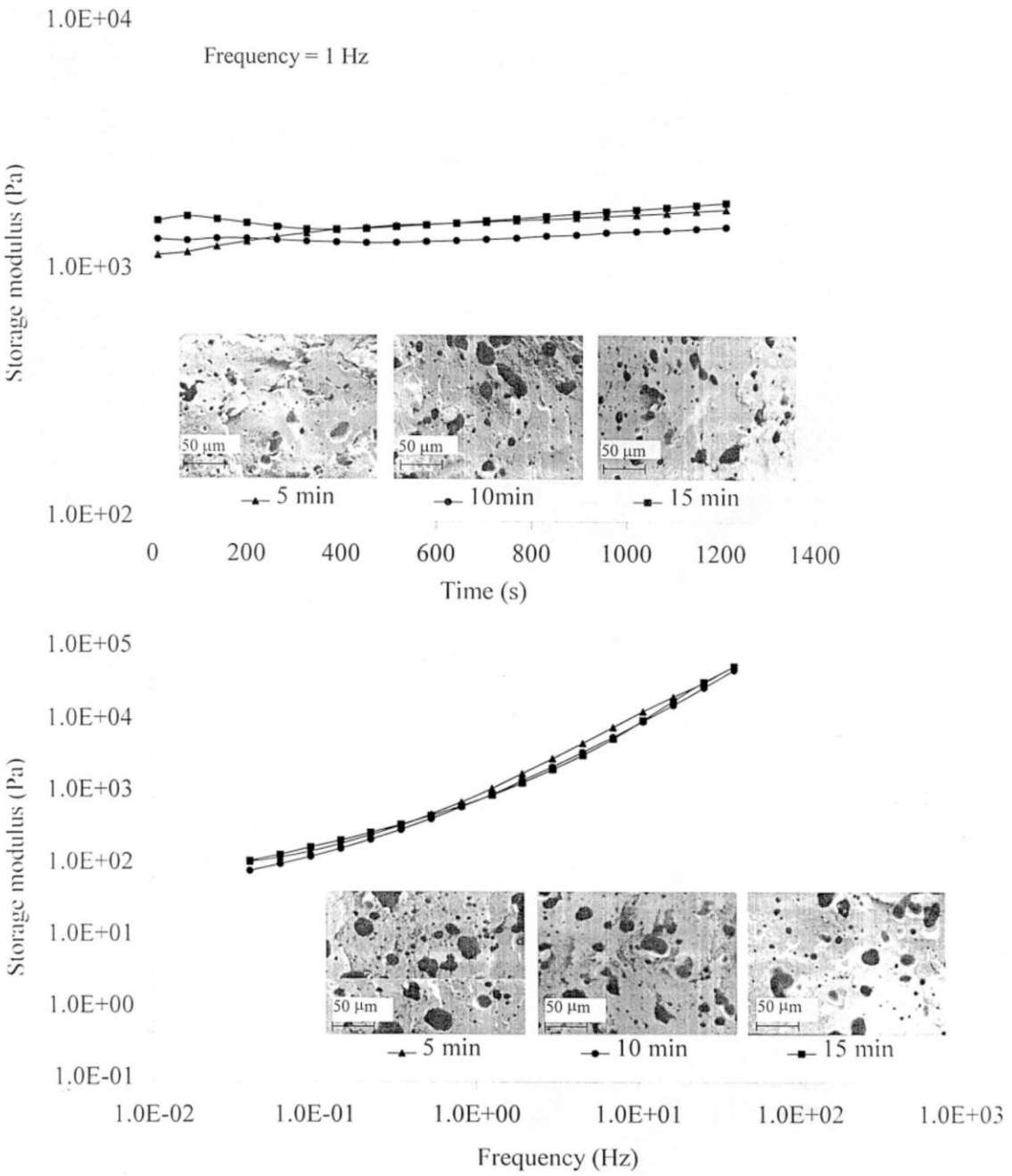

FIGURE 2. Storage modulus and SEM micrographs after rheological measurements of PA-6/EPM/EPM-g-MA blend (80/20/0, w/w/w); a) as a function of time ($\omega = 1$ Hz) and b) as a function of frequency.

and/or particle size change took place with continuing low frequency deformation. Within the experimental error, the final average particle diameters were coincident with those of the initial disks prepared with various compression molding times (Table II). Frequency sweeps (Figure 2, bottom) produced essentially the same conclusions. Similar results were obtained with reactive blends.

Results and Discussion

Our previous studies on the influence of the MA content of the rubber phase, ratio of reactive groups, and processing conditions on the chemical and morphological evolution of PA-6/EPM-g-MA blends along a co-rotating twin-screw extruder showed that a significant chemical conversion (0.50 to 0.05 wt% MA) and a dramatic decrease in the particle size of the dispersed phase (mm to μm) occurred immediately after melting as a result of the increase in interfacial area promoted by flow through the staggered kneading blocks. Further downstream the evolution becomes rather small, since with respect to morphology only a decrease in particle size distribution is significant. Moreover, the amount of PA-6/EPM-g-MA graft copolymer formed at the interface increased with increasing EPM-g-MA content, until it reached a plateau. [27] Therefore, significant variations in the rheological behavior of the blends are also anticipated immediately after melting, particularly for samples collected in ports A and B , located along the first mixing zone of the extruder (see Figure 1).

Despite the probability that morphological changes could occur during steady shear flow, capillary rheometry was used to characterize both the individual polymers and the extruded blends under conditions relevant to subsequent processing. The steady pressure readings observed should correspond to a stabilized morphology, where breakup and coalescence of the dispersed phase are balanced. The flow curves are depicted in Figure 3. At high shear rates, the viscosity of all materials is very similar. For the inert PA-6/EPM blend, the viscosity curve is similar to that of the PA-6 reference. The increase in viscosity with increasing EPM-g-MA content could be due to an increased interfacial ad-

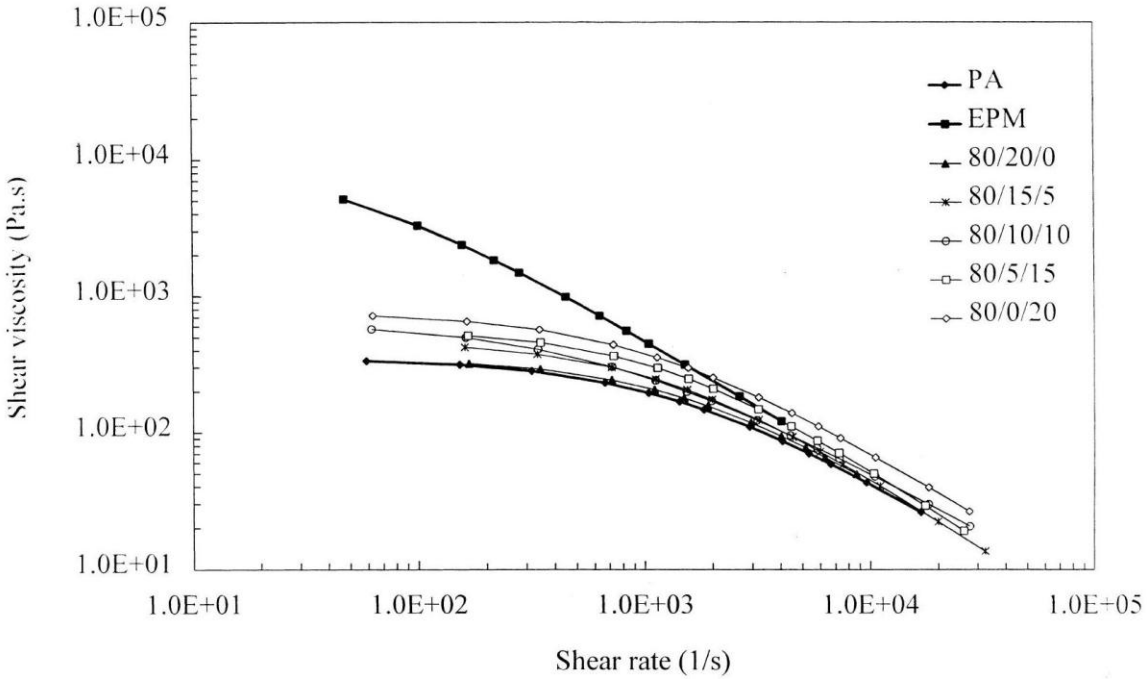

FIGURE 3. Shear flow curves of the original polymers and their extruded blends.

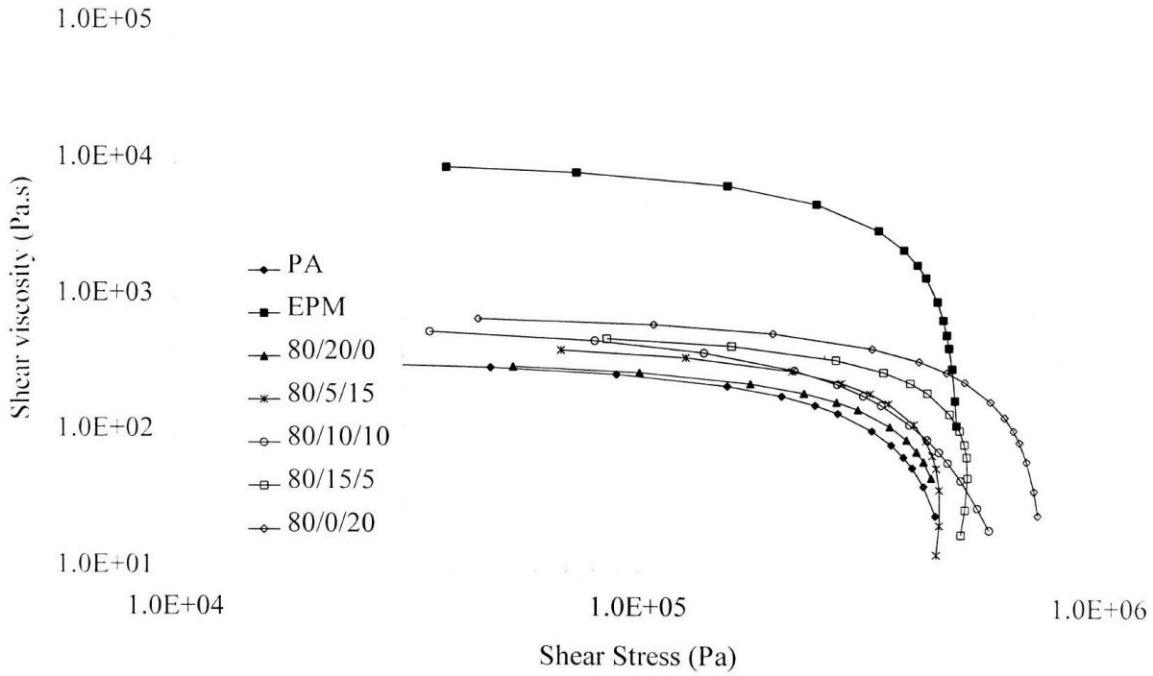

FIGURE 4. Shear viscosity vs. shear stress of the original polymers and their extruded blends.

hesion as a result of in-situ compatibilizer formation, although the flow conditions during measurement are also probably changing significantly the morphology of the dispersed phase. At the lower shear rate range, the viscosity of the blends falls between those of the components. The blends are more viscous than the reference PA-6, but less viscous than the reference rubber. Moreover, the viscosity of the blends increases with increasing MA content in the rubber phase; that is, with the amount of copolymer formed at the interface. The shape of the curves indicates that the rheology of the blends is mainly governed by the matrix, but the shift between the curves also suggests that other parameters also play a role.

The experimental data is plotted in Figure 4 in terms of apparent viscosity as a function of shear stress. The shape of the flow curves is anomalous, with the viscosity leveling off for stresses around 58×10^6 Pa. This type of behavior was initially reported for printing inks [28] and has been attributed to particle migration toward the center of the plate. [29] Earlier, Mooney and Wolstenholme [30] proposed a model for "supermolecular" flow, involving the movement and rotation of particles imbedded in the melt and causing a wall-slip-like effect. In the present case, where the flow of a melt with a higher viscosity dispersed phase develops, it appears that above a critical stress (presumably related to volume level and average size of the dispersed phase) the rubber particles will start rotating and, eventually, rolling over each other, causing a slip-like effect. Therefore, the interpretation of the data observed with capillary flow of this type of immiscible reactive blends is complex and requires special precautions.

Since oscillatory experiments preserve the morphology present before the rheological measurements, they will be used in the rest of this work. The dynamic viscosity, η', and storage modulus, G', of the original materials, PA-6, EPM, and EPM-g-MA, and of the extruded blends of PA-6/EPM (80/20, w/w) and of PA-6/EPM-g-MA (80/20, w/w) are

shown in Figure 5. The dynamic viscosities of both inert and reactive blends are always lower than those of the original components. The reactive blend is more viscous than the nonreactive blend, despite the lower viscosity of EPM-g-MA in relation to EPM, due to the formation of graft copolymer at the interface and to the fine rubber dispersion. The

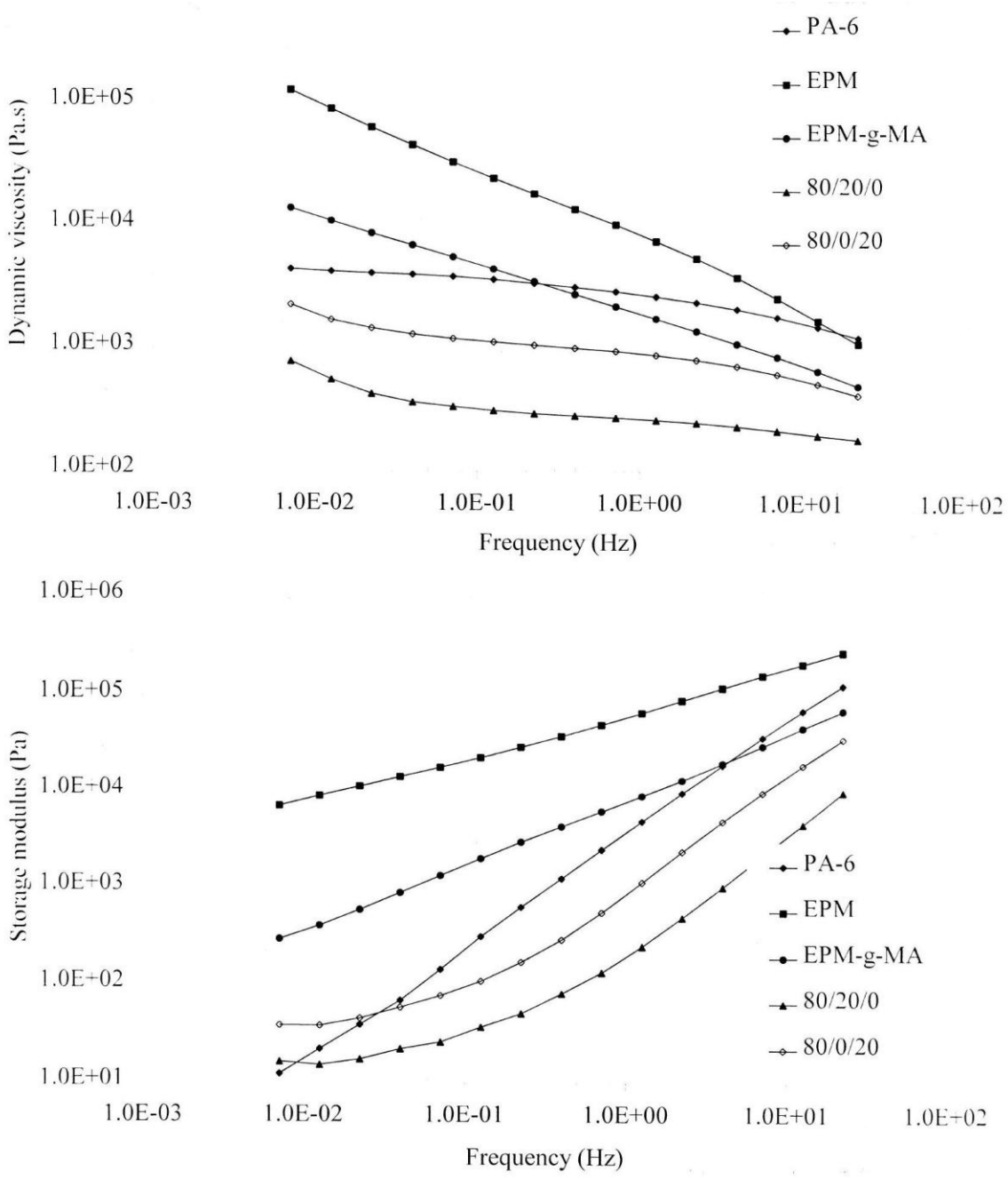

1.0E + 06

FIGURE 5. Rheological behavior of the original polymers and their blends; a) dynamic

viscosity and b) storage modulus.

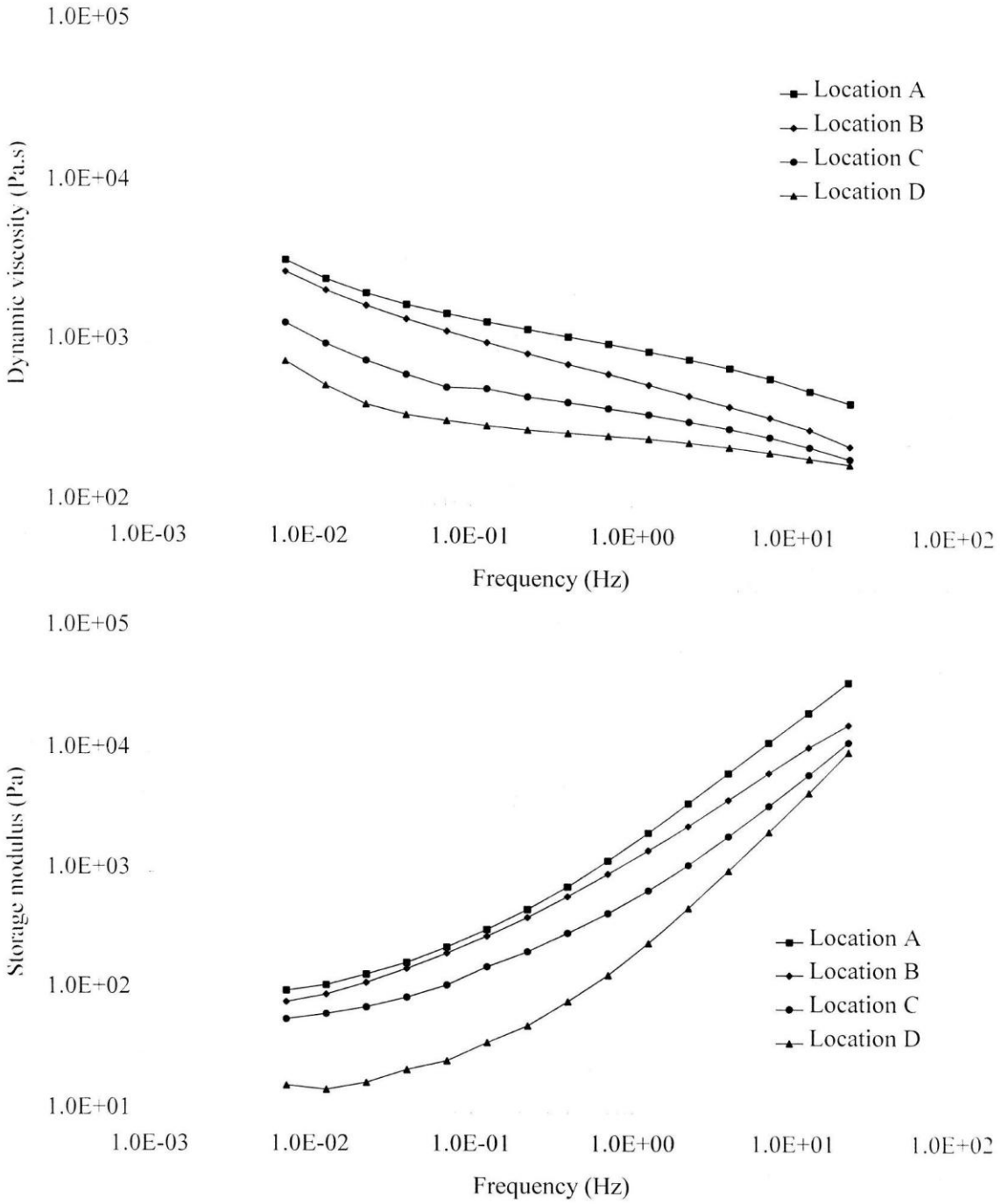

FIGURE 6. Rheological behavior of PA-6/EPM/EPM-g-MA blend (80/20/0, w/w/w) along the extruder; a) dynamic viscosity and b) storage modulus.

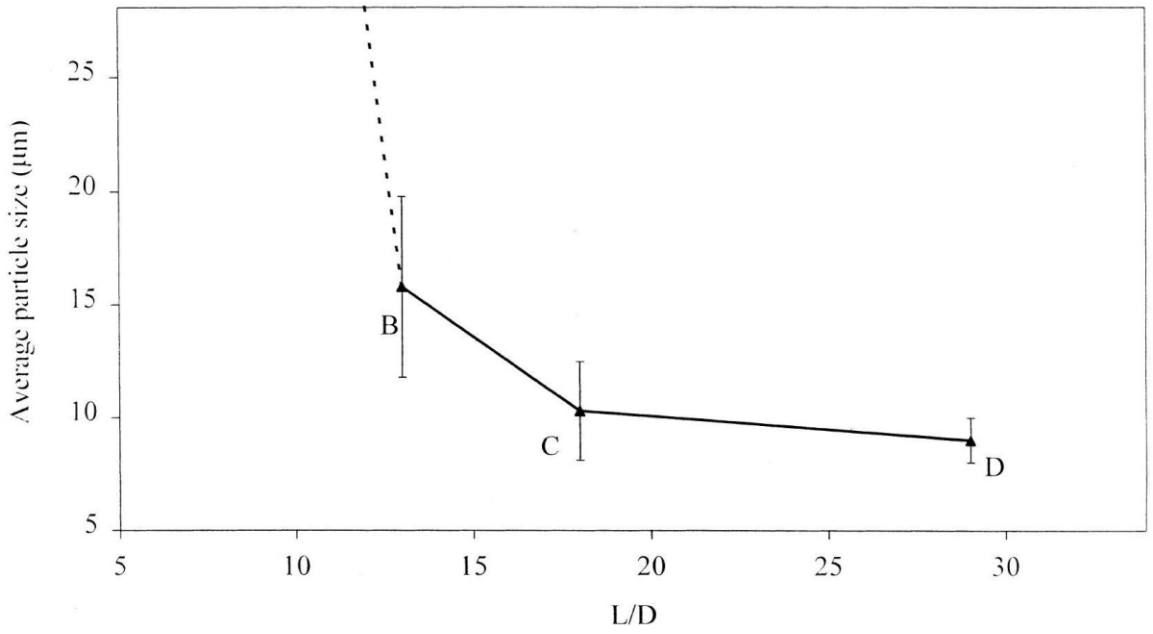

FIGURE 7. Evolution of the dispersed phase particle size of PA-6/EPM/EPM-g-MA blend (80/20/0, w/w/w) along the extruder.

trends in the elastic behavior of these materials, as indicated by G', are similar to those for η'. The increase in elasticity of the blends at low frequencies, that has frequently been reported for other systems, is also observed here and can be associated with the deformation and recovery of the dispersed rubber particles due to interfacial tension, [6,12–14] as mentioned previously. If this effect is discarded, the slopes of the η' and G' curves of the blends and of PA-6 are similar, confirming that the rheology of the blends is mainly dictated by the matrix. However, the relative magnitude of η' and G' of these materials is difficult to account for, as one would expect that the viscosity of both blends would largely fall between the values of the original materials. The study of the evolution of the rheological behavior of the various materials along the extruder could provide some insight on these phenomena.

Figure 6 shows the rheological evolution of the nonreactive PA-6/EPM (80/20, w/w) blend along the screw length. Locations A, B, and C(L/D = 12, 13, and 18 in Figure 1, respectively) correspond to screw zones where high pressure and shear were developed and location D is the extrudate. Both the dynamic viscosity and the storage modulus decrease along the extruder. In principle, this could be attributed either to changes in the dispersed phase particle size (distribution), [6,12–14] changes in interfacial structure, or to flow-induced orientation. [2,10,12] The blend morphology (average particle size) at the same locations is presented in Figure 7. The data for location A are not depicted because of the coexistence of solid and softened material. The decrease in particle size along the extruder, immediately after melting in particular (i.e., between A and B, which are only one L/D apart), and of particle size distribution, as inferred from the breadth of the standard deviation further on along the screw, seem to explain the rheological behavior. Flow-induced particle orientation was not observed.

In the case of the reactive PA-6/EPM-g-MA blend (80/20, w/w), differences between the individual η' and G′ curves are clear at lower frequencies (Figure 8), where a progressive

decrease of these parameters toward the die is observed. Differences between locations A and B are more pronounced than in the nonreactive counterpart. These results can be partially explained by the progressive decrease in particle size (distribution), as depicted in Figure 9. In our previous study, melting between locations A and B is not only completed, but the average particle size also decreases dramatically to

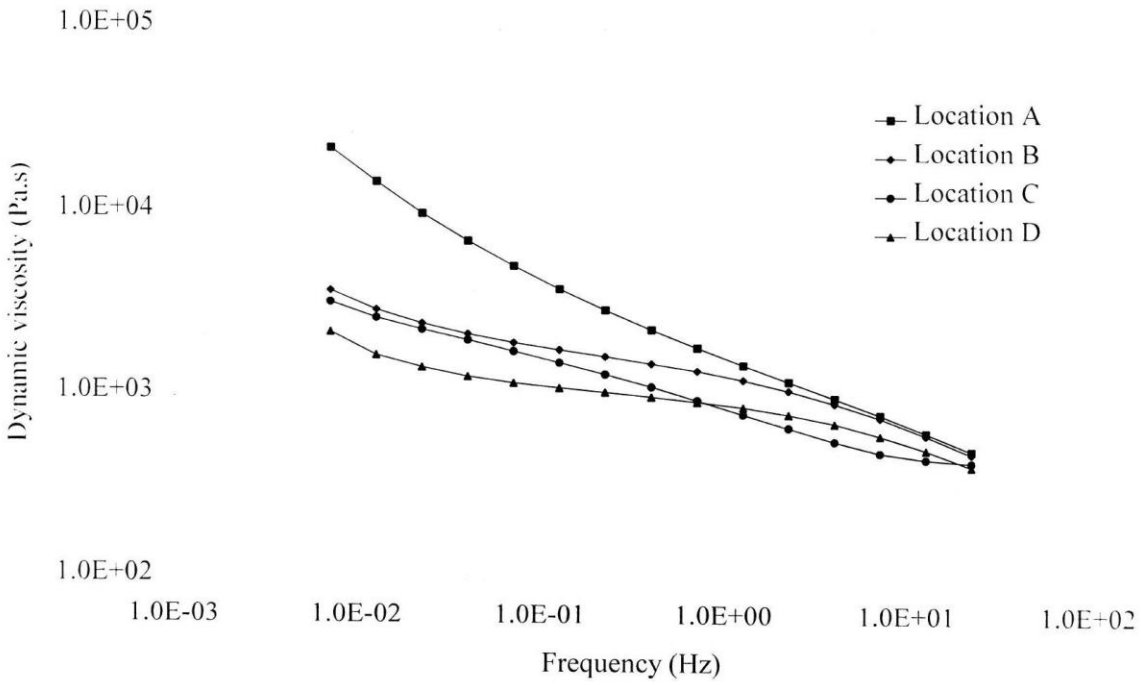

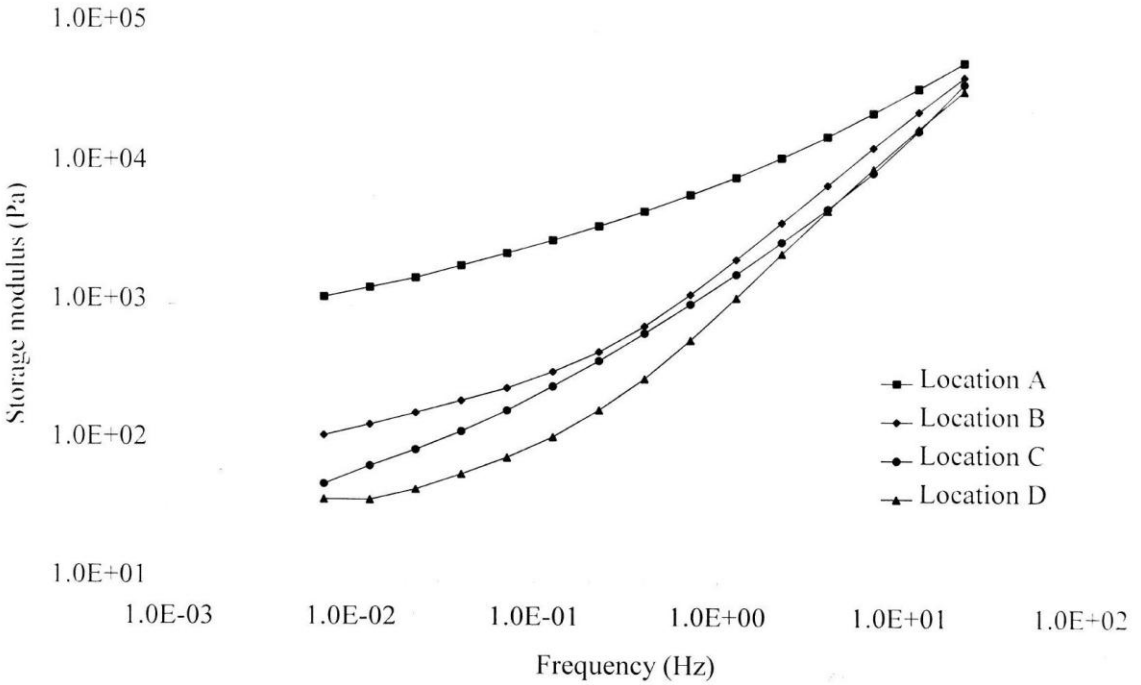

FIGURE 8. Rheological behavior of PA-6/EPM/EPM-g-MA blend (80/0/20, w/w/w) along the extruder; a) dynamic viscosity and b) storage modulus.

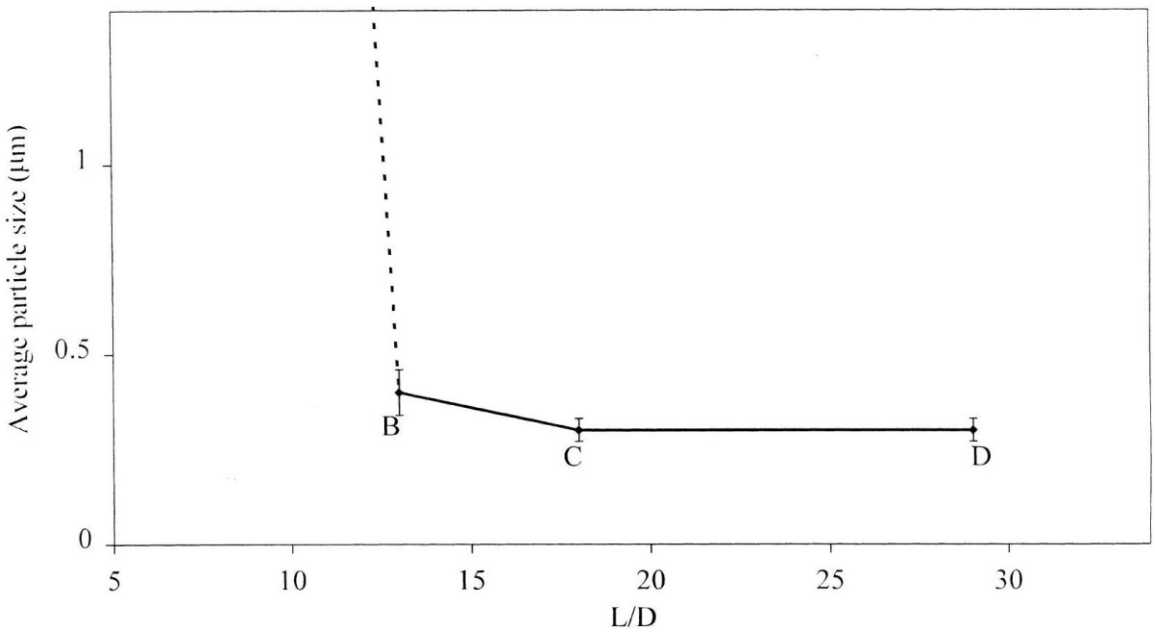

FIGURE 9. Evolution of the dispersed particle size of PA-6/EPM/EPM-g-MA blend (80/0/20, w/w/w) along the extruder.

sub-micrometer levels. TEM micrographs show a change from spherical and ribbon particles to a very regular morphology. [27] However, beyond location C no significant changes are detected.

The progressive formation of PA-6/EPM-g-MA graft copolymer at the interface would result in an increasing viscosity and elasticity. [31] Figure 10 depicts the variation of the residual MA content of the blend along the screw (determined by FT-IR of hydrochloric acid residues [27]) and of the amount of PA grafted at the interface (computed from the nitrogen content of formic acid residues). The amount of MA decreases significantly from 0.49 to 0.07% in location B and remains constant thereafter. Complete conversion of all MA groups is difficult, since the residual unreacted MA groups are probably present in the interior of the dispersed rubber particles. The amount of PA grafted at the interface increases until it reaches a plateau level at location C of about 0.8 g/ 20 g EPM + EPM-g-MA. Brahimi et al. [32] showed that η' and G' are very sensitive to the nature and volume fraction of the copolymer present at the interface (in the case of copolymer-modified PE/PS blends). In short, if the conflicting effect between decrease in particle size and progressive presence of copolymer at the interface results in the decrease of η' and G' up to location C, further downstream this continuing decrease cannot be accounted for by the same morphology/chemical conversion effects.

When PA-6 is processed as such under the same processing conditions used for the blends and its rheological behavior along the screw is also monitored, the results presented in Figure 11 are obtained. Progressive degradation (probably due to chain scission) seems to take place. This is confirmed by gel permeation chromatography, where a shift to lower

values of molecular weight is observed (the ratio Mw/Mn is 2.6 and 2.4 at locations A and D, respectively). Since the material was properly dried, the degradation of PA-6 could be related to the prescribed processing conditions/screw design used, which could promote an important viscous dissipation and, therefore, increased degradation.

In the case of the reactive PA-6/EPM-g-MA blend, matrix degradation can be even more important, since the water formed during the reaction between the PA amine end groups and the EPM-g-MA anhydride groups can hydrolyze the amide groups of the polyamide chain, increasing chain scission. In addition, the EPM-g-MA anhydride can also react with PA amide chain groups, resulting in direct degradation of the PA matrix. [21] Consequently,

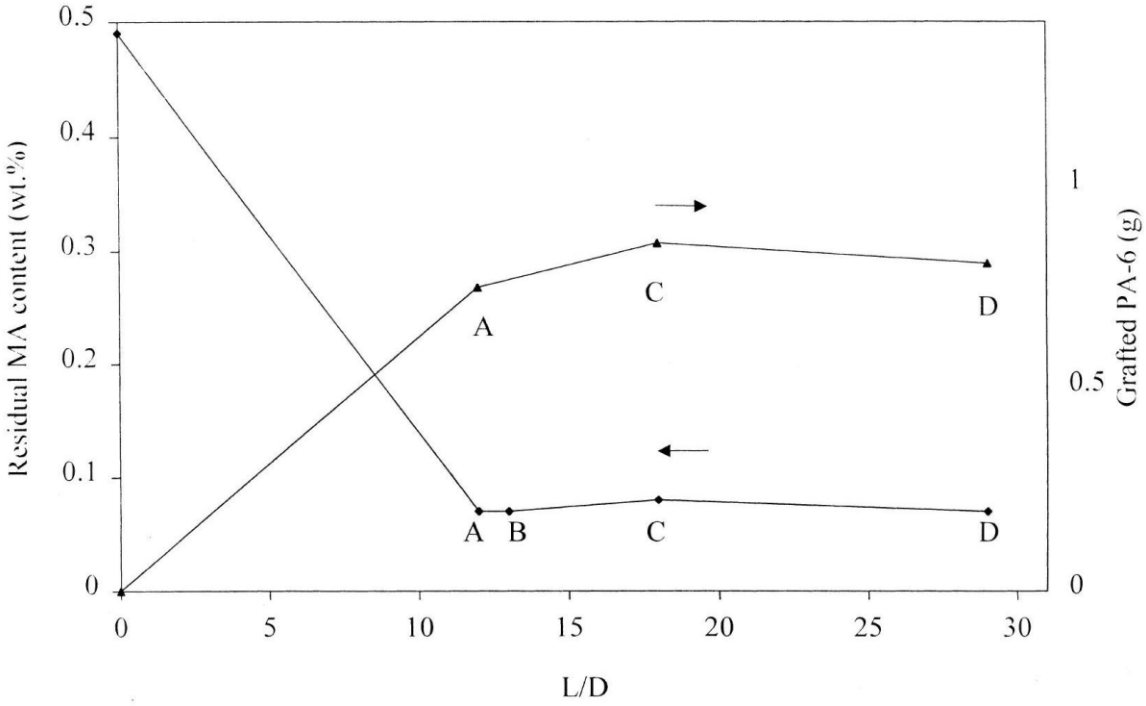

FIGURE 10. Chemical evolution (MA content and amount of grafted PA-6 on the rubber phase) of PA-6/EPM/EPM-gMA blend (80/0/20, w/w/w) along the extruder.

matrix degradation seems to play a relevant part in the rheological behavior of the blends studied in this work and accounts for the lower viscosity of the blends when compared with that of the original components (Figure 5a).

If one uses again Figure 5 for a comparison of the relative viscosity and elasticity of the various materials, a shift of the curves corresponding to PA-6 to the lower values presented in Figure 11 should be considered. The rheological behavior of the nonreactive blend would then follow closely that of PA6, thus strengthening the previous observation that the behavior of the blends studied in this work is governed by the matrix. It would be interesting to compare the experimental data with the predictions of proposed constitutive equations (e.g., by Palierne and/or Lee and Park [15,17]). Palierne derived an equation relating the complex modulus of emulsions with the viscoelasticity of both phases, the particle size and size distribution, and the interfacial tension. Lee and Park modified the Doi-Otha theory, [16] originally developed for an equal mixture of two immiscible fluids having the same viscosity

and density, to account for a mismatch in the viscosities and to consider three different mechanisms of relaxation: coalescence, shape relaxation, and breakup by interfacial tension. Unfortunately, the morphology type (dispersed particles in a less viscous matrix), the presence of occlusions of PA-6 in the dispersed rubber particles, and the matrix degradation jeopardize the applicability of these models establishing the relationship between morphology and rheology.

The effect of the EPM-g-MA content on the rate of morphology and chemical conversion along the extruder is illustrated in Figures 12 (location A) and 13 (location D). As could be anticipated from the previous discussion, both the dynamic viscosity and the storage modulus increase with increasing volume fraction of the graft copolymer formed at the interface. This is in accordance with previous results, [27] showing that the amount of PA-6 grafted at the interface increases with increasing MA content of the rubber phase. The anticipated lower viscosity and elasticity of the extrudate (location D) result, as discussed previously, from the combined

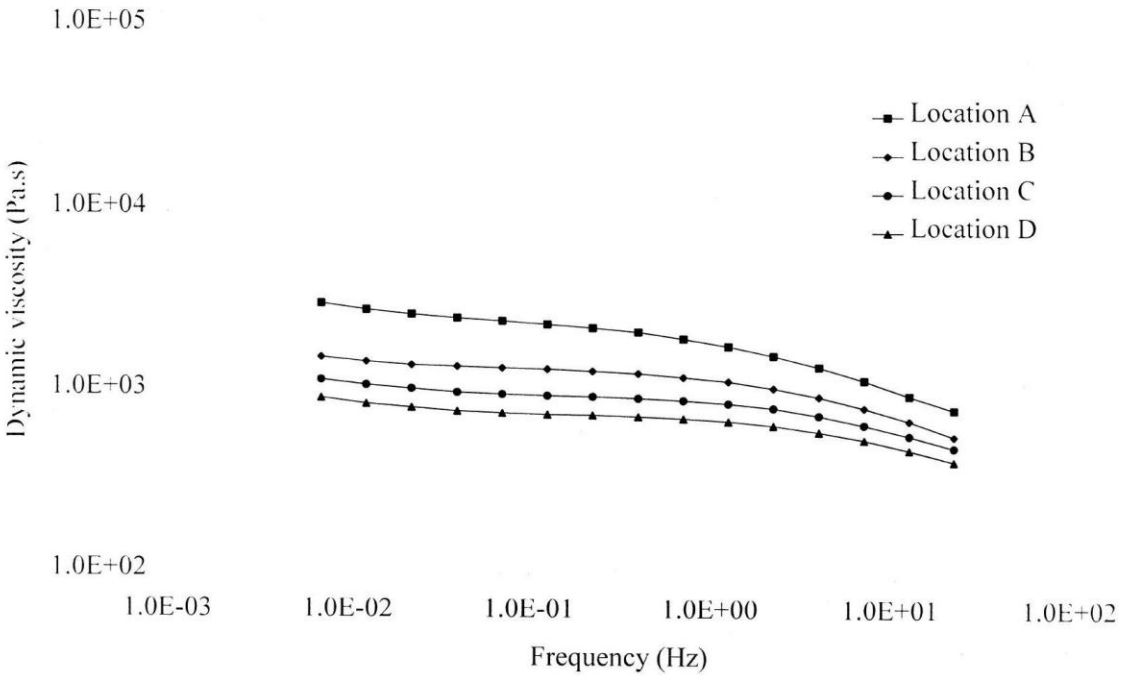

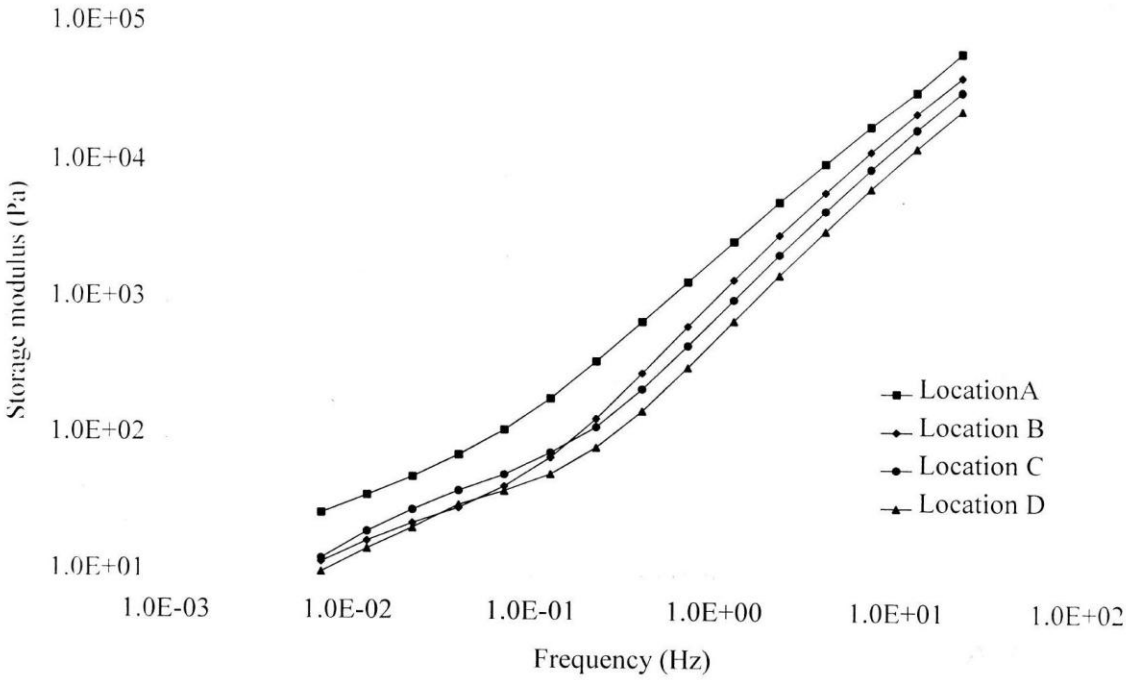

FIGURE 11. Rheological behavior of PA-6 along the extruder; a) dynamic viscosity and b) storage modulus.

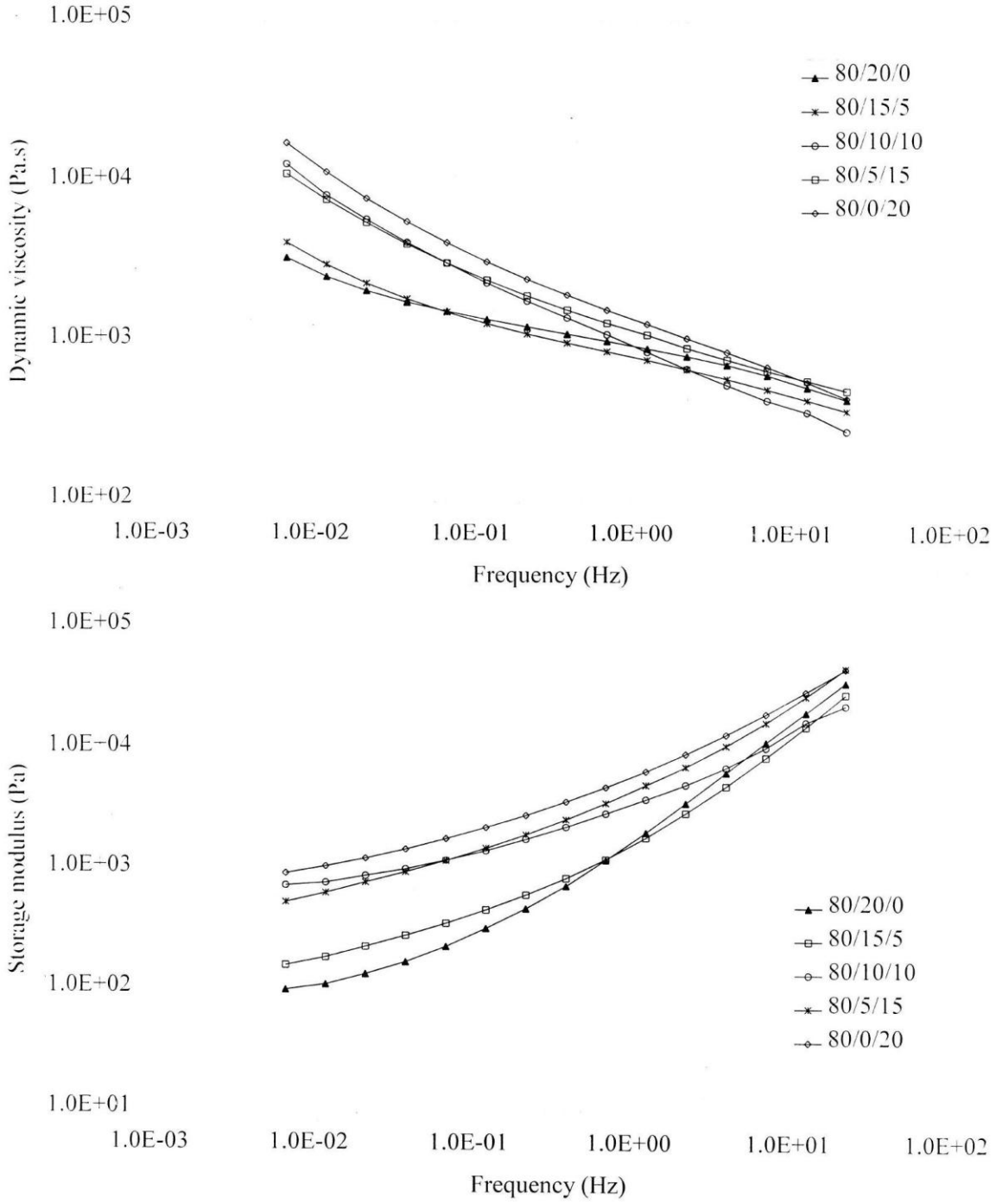

FIGURE 12. Rheological behavior of blends with different compositions at location *A*; a) dynamic viscosity and b) storage modulus.

1.0E + 05

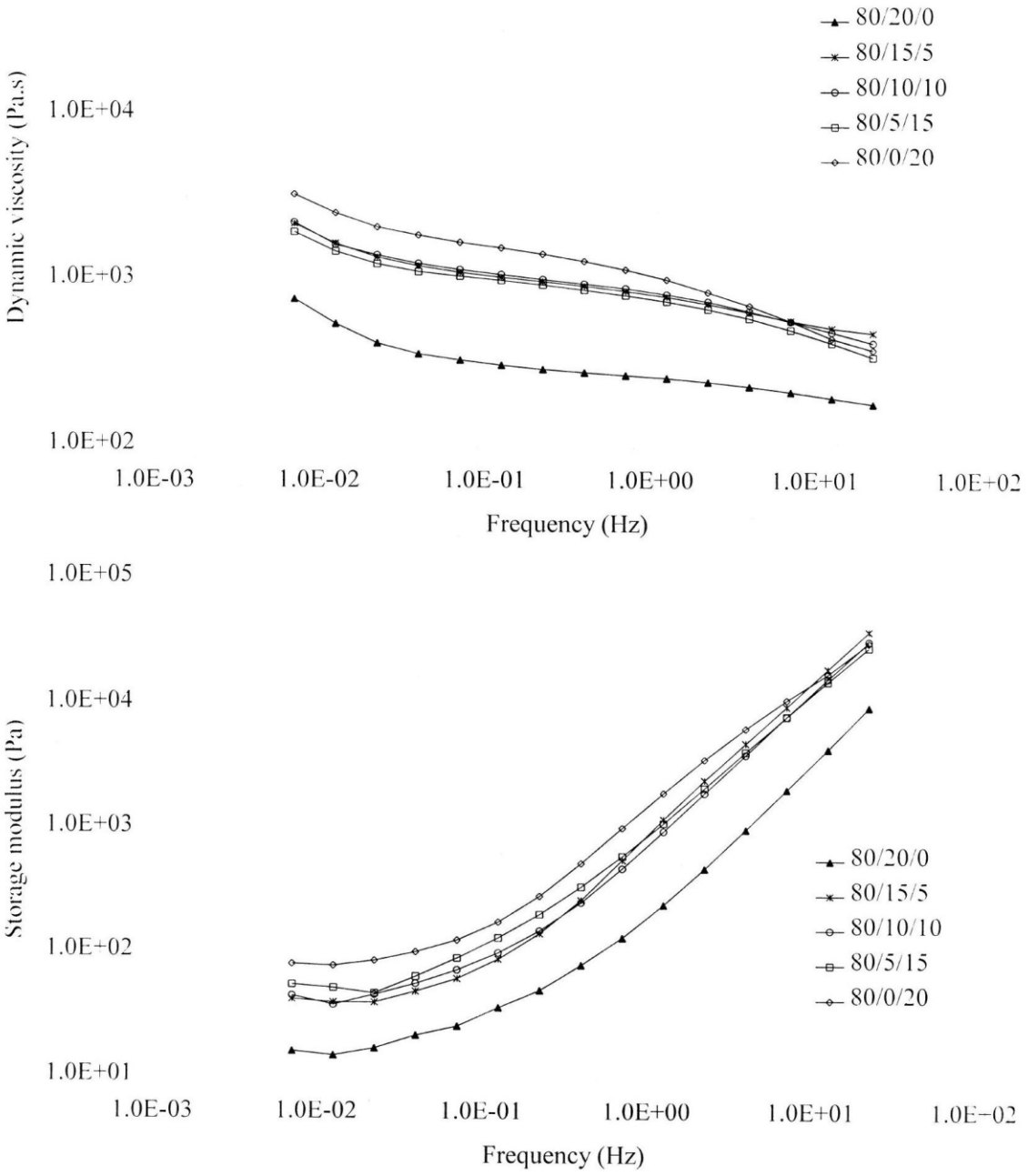

FIGURE 13. Rheological behavior of blends with different compositions at location *D*; a) dynamic viscosity and *b*) storage modulus.

effects of morphology, chemical conversion, and matrix degradation.

Conclusions

This work showed that the linear viscoelastic behavior of immiscible noncompatibilized and compatibilized polyamide-6/rubber blends along a twin-screw extruder is related to changes in morphology and/or formation of the in-situ compatibilizer. The dynamic viscosity and the storage modulus decrease substantially upon melting of the components,

since this process is induced by a significant increase in interfacial area. However, the rheological data could not be analyzed making use of available theoretical models (proposed, among others, by Palierne and Lee and Park), due to morphology type and matrix degradation. In fact, the phenomenon of matrix degradation explains the relatively low viscosity levels of the blends, when compared with those of the original materials.

These results confirm that rheology can be a powerful method for probing the morphology development of immiscible polymer blends. The development of in- and on-line measurements should therefore be pursued, given their potential for realtime monitoring and control of blend preparation under industrial conditions. This work is currently in progress. [33]

Acknowledgments

The authors are grateful to DSM, the Netherlands, for materials and technical support; to Exxon (Spain) for materials; and to INVOTAN, Portugal for funding the project. The assistance on the rheological measurements and the profitable discussions with our colleague João Maia are also gratefully acknowledged.

References

2. Utracki, L. A. Polymer Alloys and Blends; Hanser Publishers: New York, 1990.
3. Utracki, L. A., Ed. Two-phase Polymer Systems; Hanser Publishers: New York, 1991.
4. Utracki, L. A. Encyclopaedic Dictionary of Commercial Polymer Blends; ChemTec Publishing: Toronto, 1994.
5. Datta, S.; Lohse, D. Polymeric Compatibilizers; Hanser Publishers: New York, 1996.
6. Bousmina, M.; Muller, R. Rheol Acta 1996, 35, 369.
7. Kitade, S.; Ichikawa, A.; Imura, N.; Takahashi, Y.; Noda, I. J Rheol 1997, 5, 1039.
8. Nielsen, L. Polymer Rheology; Marcel Dekker: New York, 1977.
9. Xanthos, M.; Tan, V.; Ponnusamy, A. Polym Eng Sci 1997, 37, 1102.
10. Lacroix, C.; Gamela, M.; Carreau, P. J. J Rheol 1998, 42, 41.
11. Vinckier, I.; Moldenaers, P.; Mewis, J. J Rheol 1996, 40, 613.
12. Lacroix, C.; Aressy, M.; Carreau, P. J. Rheol Acta 1997, 36, 416.
13. Grizzuti, N.; Bifulco, O. Rheol Acta 1997, 36, 406.
14. Bouilloux, A.; Ernest, B.; Lobbrecht, A.; Muller, R. Polymer 1997, 38, 4775.
15. Palierne, J. F. Rheol Acta 1990, 29, 204.
16. Doi, M.; Ohta, T. J Chem Phys 1991, 95, 1242.
17. Lee, H. M.; Park, O. J Rheol 1994, 38, 1405.
18. Memon, N. A.; Muller, R. J Polym Sci Part B: Polym Physics 1998, 36, 2623.
19. Scott, C. E.; Macosko, C. W. Polym Eng Sci 1995, 24, 1938.
20. Borggreve, R. J. M.; Gaymans, R. J. Polymer 1989, 30, 63.
21. van Duin, M.; Aussems, M.; Borggreve, R. J. M. J Polym Sci Part A: Polym Chem 1998, 36, 179.
22. Cartier, H.; Hu, G. H. Proc. Polyblends 97; Boucherville, Canada, 1997.
23. Scholz, P.; Froelich, D.; Muller, R. J Rheol 1989, 33, 481.
24. Sakai, T. Adv Polym Techn 1995, 14, 277.
25. Esseghir, M.; Yu, D.; Gogos, C.; Todd, D. Proc SPE ANTEC; Indianapolis, IN 1996.
26. Machado, A. V.; Covas, J. A.; van Duin, M. J Appl Polym Sci 1999, 71, 135.
27. Machado, A. V.; Covas, J. A.; van Duin, M. J Polym Sci Part A: Polym Chem 1999, 31, 1311.

28. Gregory, T.; Mayers, S. Surf Coat Int 1993, 76, 82.
29. Barnes, H. A. J Non-Newton Fluid Mech 1995, 56, 221.
30. Mooney, M. J Appl Phys 1958, 25, 1098.
31. Germain, Y.; Ernst, B.; Genelot, O.; Dhamani, L. J Rheol 1994, 38, 681.
32. Brahimi, B.; Ait-Kadi, A.; Ajji, A.; Jerôme, R.; Flat, R. J Rheol 1991, 35, 1069.
33. Covas, J. A.; Nobrega, J. A.; Maia, J. M. Polym Testing 2000, 19, 165.